

Magnetic Phases and Specific Heat of Ultra-Thin Holmium Films

L.J. Rodrigues,

*Departamento de Física Teórica e Experimental,
Universidade Federal do Rio Grande do Norte, Natal - RN 59600-900, Brazil*

V.D. Mello

Departamento de Física, Universidade do Estado do Rio Grande do Norte, Mossoró - RN 59625-620, Brazil

D.H.A.L. Anselmo

*Departamento de Física Teórica e Experimental,
Universidade Federal do Rio Grande do Norte, Natal - RN 59072-970, Brazil*

M.S. Vasconcelos*

Escola de Ciência e Tecnologia, Universidade Federal do Rio Grande do Norte, 59072-970, Natal- RN, Brazil

(Dated: March 25, 2021)

We report model calculations of the magnetic phases of very thin Ho films in the temperature interval between 20K and 132K, and show that slab size, surface effects and magnetic field due to spin ordering may impact significantly the magnetic phase diagram. There is a relevant reduction of the external field strength required to saturate the magnetization and for ultra-thin films the helical state does not form. We explore the heat capacity and the susceptibility as auxiliary tools to discuss the nature of the phase transitions.

PACS numbers: 75.50.Cc, 73.22.-f, 75.40.-s

Keywords: Magnetic phases, nanofilms, specific heat

I. INTRODUCTION

Nowadays, rare earths are vital to some of the world's fastest growing markets: clean energy and high technology (for a review, see [1], and references therein). They are found in most everyday applications because of their unique chemical and physical properties. New applications have arisen consistently over the past 50 years, including important environmental innovations such as catalytic converters and the development of permanent magnets which have enabled greater efficiency, miniaturization, durability and speed in electric and electronic components. Generally they are classified into one of two categories, namely, light rare earths and heavy rare earths, with varying levels of uses and demand on the industry technologies. For example, the lanthanum is a light rare earth responsible for making rechargeable lanthanum nickel metal in hydride batteries [2] used in electric and hybrid vehicles, laptops, cameras, etc. Also it is used to improve visual clarity in camera lenses, telescopes and binoculars. Also, in optical fibres it increase significantly the transmission rates. Another heavy rare earth is the Dysprosium [3], most commonly used in the manufacture of neodymium-iron-boron high strength permanent magnets. Dysprosium is used in radiation badges to detect and monitor radiation exposure. However, the

applications in spin wave magnetic devices is yet scarce.

One of most recent purposes is the use of these materials in solid-state rare-earth-ion-doped systems, which justifies their status as very strong candidate to a long-lived quantum memory system [4]. Also, very recently, Lovric et al. [5], have reported a high fidelity optical memory, made of a rare earth doped crystal, in which dynamical decoupling is used to extend the storage time. It is notable, until we know, the lack of studies about the magnetic phases in rare earth. With this work we intend to fill some part of this lack with the study of the magnetic phases of rare-earth thin films, aiming further applications.

Magnetic ordering in the heavy rare-earth lanthanides [6] is mediated by the RKKY interaction in which the polarization of conduction electron yields an indirect exchange between localized 4f moments on neighboring lattice sites. The interplay between this long-range interaction and anisotropic and magneto-crystalline effects results in complex magnetic ordering and the possibility of a variety of magnetic structures. As stated before, understanding the magnetism of thin films is of general importance in a technological context, and rare-earth metals are used in a wide, range of applications, and have attained global economics importance [7, 8]. Among the rare-earths, Holmium in particular displays unusual behavior which, coupled with the large temperature stability of the intermediate helimagnetic phase when compared to Dy and Tb, has led to it being treated as a model system in a number of recent experimental [9] and

¹ Phone: +55 84 3342 2355; Fax: +55 84 3215 3791

* manoevasconcelos@yahoo.com.br; mvasconcelos@ect.ufrn.br

theoretical [10] studies. In the bulk, Holmium metal orders magnetically below $T_N=132\text{K}$ (Néel temperature) and the moments in consecutive neighboring basal planes rotate to give a long-period helical phase. At temperatures below $T_C=20\text{K}$ (Curie temperature) it arranges as a cone with angle of $80.5^\circ \leq \theta \leq 90^\circ$, giving rise to a conical phase. When a magnetic field is applied in the basal plane other magnetic structures are observed including a basal plane ferromagnetic phase, fan phase and helifan phase [11, 12]. In thin films when the thickness is comparable with the periodicity of the ordered structure, is expect that even the magnetic arrangement itself can be strongly modified. For ultrathin films, however, as the number of spin layers is reduced by decreasing the film thickness, additional structures are established including a fan structure and a spin-slip configuration, highlighting the importance of surface and interfacial effects [13]. This finite-size effect is caused by the reduced number of atoms in the direction perpendicular to the film plane that leads to a decrease of the total magnetic exchange energy. Rare-earth helimagnets such as Ho, Dy, and Tb (for a review see [13]) represent the best candidates to put into evidence such finite-size effects.

This paper is organized as follows. In Sec. II we provide our theoretical framework for the Hamiltonian, which takes into account the hexagonal anisotropy. A discussion about our model and comparison with other works are done in Sec. II. Finally, we summarize our main conclusions in Sec. IV.

II. THEORETICAL MODEL

We investigate a *c*-axis thin film, consisting of a stacking of atomic layers with equivalent spins, infinitely extended in the *x*-*y* directions. The spins in each monolayer are exchange coupled with the spins in the first and second neighbor monolayers. The anisotropy is uniform throughout the film and the near surface spins have reduced exchange energy. The magnetic Hamiltonian is given by:

$$\begin{aligned}
 H = & J_1(g-1)^2 \sum_{n=1}^{N-1} \vec{J}(n) \cdot \vec{J}(n+1) + \\
 & J_2(g-1)^2 \sum_{n=1}^{N-2} \vec{J}(n) \cdot \vec{J}(n+2) + \\
 & \sum_{n=1}^N \left[K_6^6 \cos(6\varphi_n) - g\mu_B \vec{J}(n) \cdot \vec{H} \right]
 \end{aligned} \quad (1)$$

In Eq. (1), J_1 and J_2 describe the exchange interaction between the nearest and next nearest monolayers, $\vec{J}(n)$ denotes the total angular momentum per atom in the n -th monolayer. K_6^6 describes the hexagonal anisotropy and the last term is the Zeeman Energy, where the external field, \vec{H} , is applied in one easy direction in the

hexagonal plane, making an angle of 30° with *x* axis. Also, $K_6^6(T)$ is adjusted so as to reproduce the temperature dependence [17] of the hexagonal anisotropy energy. We use the Ho bulk energy parameters [15], where $J=8$, $J_1 = 47k_B$, $J_2 = -J_1/4 \cos \phi(T)$, where $\phi(T)$ is the temperature dependent helix turn angle [16]. Also, $g = 5/4$ is the Landé factor, corresponding to a saturation magnetic moment per atom of $9.5\mu_B$. We use a self-consistent local field model that incorporates the surface modifications in the exchange field and the thermal average values ($\langle J(n) \rangle$; $n = 1; \dots N$) and the orientation of the spins in each layer ($\langle \phi_n \rangle$; $n = 1; \dots N$) [18, 19].

III. RESULTS AND DISCUSSION

In this paper we will concentrate our analysis mainly on the phase diagrams $H-T$ obtained for Holmium bulk and for the films composed by $n=24, 10$ and 7 monolayers. We present the $H-T$ diagram in the temperature interval from 20K to 132K . The magnetic phase transitions are function of the external magnetic field H , temperature T , and thickness N . We use the specific heat (magnetic and lattice contributions), and the magnetic susceptibility to identify the nature of the magnetic phase transition.

In the absence of external magnetic field the Ho bulk film arranges in helimagnetic form from 20K (T_C , Curie temperature) to 132K (T_N , Néel temperature). In Fig.(1) we show the $H-T$ diagram of Ho bulk where, increasing the field in the isothermal process there is a phase transition from helimagnetic phase to fan phase, going to ferromagnetic phase: Helix→Fan→FM. For heating process (and isofield process), we can see up to four transitions. For example, at 8kOe : (FM→Fan→Helix→Fan→PM).

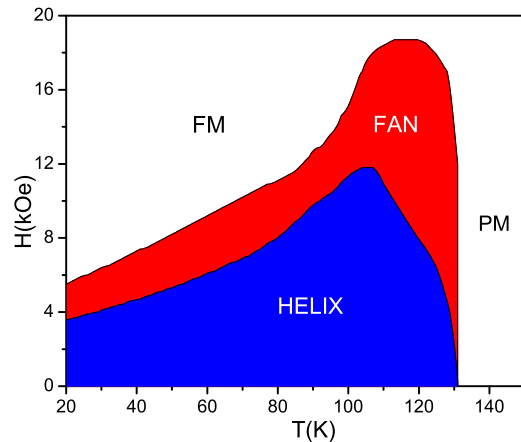


Figure 1. Phase diagram of Ho bulk.

In the Fig.(2) we show the dependence of isothermal magnetization with applied magnetic field, for both $T=50\text{K}$ and 70K . The magnetic susceptibility (*inset*) for selected values of magnetic field and temperatures is also presented. We can identify in the phase diagram, that

for $T=50\text{K}$ and $T=70\text{K}$ there are two magnetic phase transitions: Helix \rightarrow Fan \rightarrow FM. For $T=50\text{K}$ we can see a peak in the magnetic susceptibility in $H=5\text{kOe}$ marking the magnetic phase transition, Helix \rightarrow Fan and Fan \rightarrow FM in $H=7.5\text{kOe}$

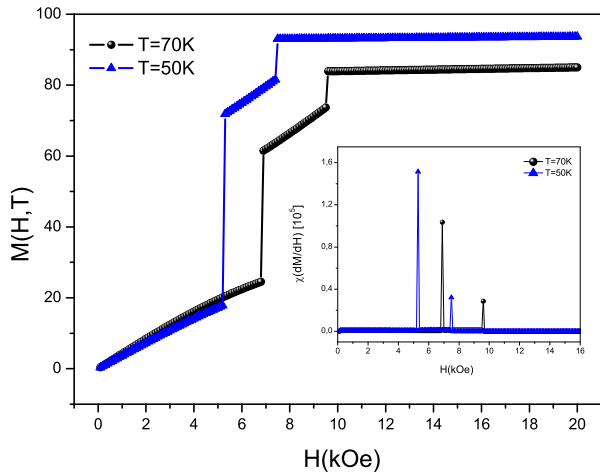


Figure 2. Isothermal magnetization for $T=50\text{K}$ and 70K . *Inset*: Magnetic susceptibility for $T=50\text{K}$ and 70K .

The specific heat is also investigated, as shown in Fig.(3), for selected values of magnetic field, where both magnetic and elastic (lattice) contributions are considered. We can see that for $H=6\text{kOe}$, the magnetic phase transitions are marked by the specific heat. The FM \rightarrow Fan phase magnetic transition is marked by a deep peak. The Fan \rightarrow Helix transition exhibit a small plateau in the specific heat. It is followed by a peak in the Helix \rightarrow Fan phase magnetic transition and by a drop in the Fan \rightarrow PM magnetic phase transition. The peak in specific heat, close to T_N , shows the magnetic phase transition, Fan \rightarrow PM, followed by a drop in the curve due to lattice contributions. However, the specific heat measurements in weak magnetic fields do not mark all magnetic phase transitions, because the field interval which destabilizes the magnetic order is low, therefore, it is more appropriate to resort to measurements of magnetic susceptibility for fields in that interval.

In Fig.(4-a) we show the H - T diagram, describing the magnetic phases for a Ho film consisting of 24 monolayers. In principle, the thickness is enough for two helix with turning angle of 30° . But in this case the magnetic phase diagram is different from the one in bulk. We can see that the presence of surface induces new magnetic phases compared with Ho bulk. This occurs because the surface spins align more easily with the easy axis of the hexagonal anisotropy than spins from inner atomic layers, due to the reduced exchange field in the surface region.

The helifan phase is clearly induced by surfaces. There is a threshold thickness for the stabilization of the helifan magnetic phase. We can see that there is a short region in the diagram referring to the helifan phase in

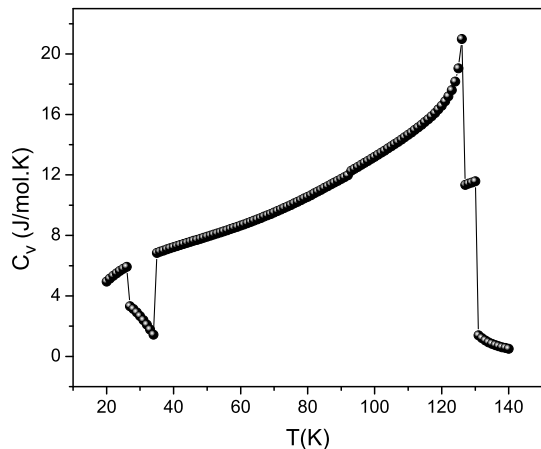


Figure 3. Specific Heat of Ho bulk for $H=6\text{kOe}$. Several magnetic phase transitions are observed.

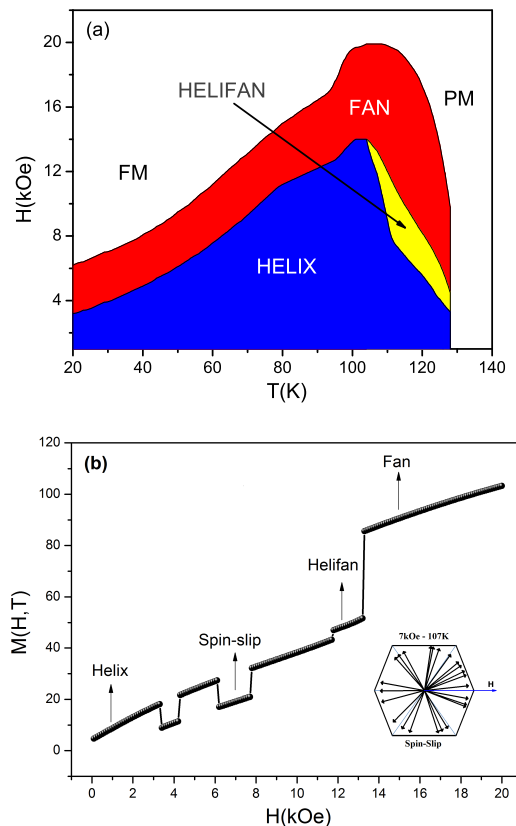


Figure 4. (a) Phase diagram of Ho films with 24 monolayers. (b) Isothermal magnetization for $T = 107\text{K}$. *Inset*: Spin-slip structure for $T = 107\text{K}$ and 7kOe .

the temperature interval from $T=103\text{K}$ to 128K and the magnetic field interval from $H=3\text{kOe}$ to 13.5kOe .

In Fig.(4-b) we can identify six magnetic phase transitions. The curve shows four peaks in $H=3.1\text{kOe}$, $H=4\text{kOe}$, $H=6\text{kOe}$ and $H=7.8\text{kOe}$ for the magnetic phase transitions Helix \rightarrow spin-slip and spin-slip \rightarrow Helix. Also,

we can see two peaks at $H=11.8\text{kOe}$ and $H=13\text{kOe}$ for the magnetic phase transitions Helix \rightarrow Helifan and Helifan \rightarrow Fan, respectively. The last phase transition, Fan \rightarrow FM, is marked by a small plateau in $H=20\text{kOe}$ (not shown in the figure). In the inset we illustrate how the magnetic moments arrange in the spin-slip magnetic structure, for $T=107\text{K}$.

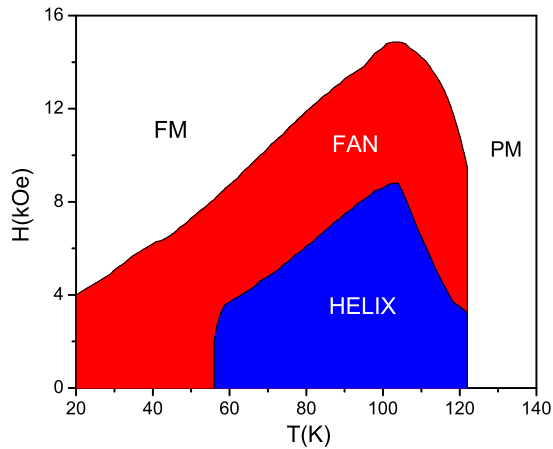


Figure 5. Phase diagram of Ho films with 10 monolayers.

Our results evince that in ultrathin Ho films ($N < 10$ monolayers), the helimagnetic phase is not stabilized. We can see in Fig.(6) that for ultrathin films the interval of magnetic field, which leads to a phase transition, is smaller than the interval of magnetic field in Ho bulk and thick Ho films. In this case the specific heat measure may be not a good tool for the identification of the magnetic phase transition. Also, from the Figs. (4-a), (5), and (6), we can observe the appearing of the helifan phase, as we increase the number of monolayers. Also, as we have commented above, this is a surface- induce effect. This effect is expected for this type of magnetic thin films, as it was reported in other works [18, 19]. With the increasing of the number of monolayers ($N \gg 1$) this helifan phase will disappear, recovering the H - T diagram of Ho in bulk, as in Fig. (1).

IV. CONCLUSION

In conclusion, we have studied the magnetic phases of very thin Ho films in the temperature interval between 20K and 132K. The present study shows the strong influence that the surface and thickness of a thin film

(See Figs. (4), (5), and (6)), associated with the existing competition between the energies of exchange and magneto-crystalline anisotropy, exerts on the magnetic order of these systems, when in the presence of an external magnetic field and temperature. The slab size, surface effects and magnetic field due to spin ordering impact significantly the magnetic phase diagram. Also, the presence of an external field gives rise to the magnetic phase Fan and the spin-slip structures observed in

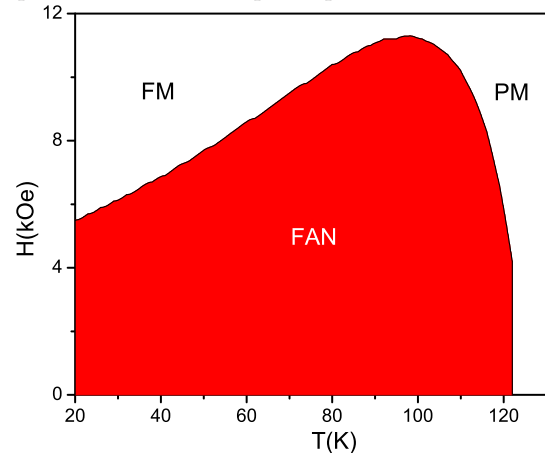


Figure 6. Phase diagram of Ho films with 7 monolayers.

Ho originates from the anisotropy competition between magnetic hexagonal and energy exchange energies, causing a significant change in the magnetic symmetry of the system (Figs 1-6). Specifically, the helifan phase emerges due to the presence of surfaces, and to a limit where the film thickness is twice the period of the helix of the film and have a strong planar anisotropy of the same order of magnitude of the exchange energy (Fig. 4). The specific heat curves is presented, which consider both magnetic and elastic (lattice) contributions. From Fig. (2) we can see that all magnetic phase transitions, for strong enough magnetic fields, are marked by the specific heat. Here we emphasize that the specific heat measurements in weak magnetic fields do not mark all magnetic phase transitions, because the field interval that destabilizes the magnetic order is low, so we consider the magnetic susceptibility measurements as more appropriate phase markers, for this interval of fields.

ACKNOWLEDGMENTS

The authors acknowledge the financial support from the Brazilian research agencies CNPq and FAPERN.

[1] F. Ronning and S. Bader, J. Phys.: Condens. Matter **26**, 060301(2014).

[2] K. Binnemans, P.T. Jones, B. Blanpain, T.V. Gervenc , Y. Yang, A. Waltone , M. Buchertf, Journal of Cleaner Production 51, 1 (2013).

- [3] D. N. Brown, Z. Wu, F. He, D. J. Miller and J. W. Herchenroeder, *J. Phys.: Condens. Matter* **26**, 064202 (2014).
- [4] N. Timoney, I. Usmani, P. Jobez, M. Afzelius, N. Gisin, arXiv:1301.6924 [quant-ph] (2013).
- [5] M. Lovric, D. Suter, A. Ferrier, and P. Goldner, *Phys. Rev. Lett.* **111**, 020503 (2013).
- [6] W.C. Koehler, in *Magnetic Properties of Rare Earth Metals*, (Ed. R.J. Elliott, Plenum Press, London 1972, p. 81).
- [7] U.S. Environmental Protection Agency. EPA 600/R-12/572, Cincinnati, OH. Retrieved from www.epa.gov/ord (2012)
- [8] Fight for Rare Earth, Reuters Special Edition, november (2010).
- [9] E. Weschke, H. Ott, E. Schierle, C. Schubler-Langeheine, D.V. Vyalikh, and G. Kaindl, *Phys. Rev. Lett.* **93**, 157204 (2004).
- [10] F. Cinti, A. Cuccoli, and A. Rettori, *Phys. Rev. B.* **78**, 020402(R) (2008).
- [11] J. Jensen and A.R. Mackintosh, *Phys. Rev. Lett.* **64**, 2699 (1990).
- [12] J. Jensen and A.R. Mackintosh, *Journal of Magnetism and Magnetic Materials.* 104-107, 1481 (1992).
- [13] J. Jensen and A.R. Mackintosh, in *Rare Earth Magnetism.*, (Oxford University Press, Oxford, 1991).
- [14] V.D. Mello, A.L. Dantas and A.S. Carriço, *Solid State Communications.* **140**, 447 (2006).
- [15] S. Legvold, in *Rare Earth Metals and Alloys.*, (North-Holland Publishing Company, 1980).
- [16] A.M. Venter and P.V. Plessiz, *J. Phys. Cond. Matter*, **9** 5167 (1997).
- [17] B. Coqblin, in *The Electronic Structure of RareEarth Metals and Alloys: the Magnetic Heavy Rare-Earths*, (Academic Press, New York, 1977).
- [18] V.D. Mello, A.S. Carriço and N.S. Almeida, *Phys. Rev. B* **59**, 6979 (1999).
- [19] V.D. Mello and A.S. Carriço, *Surf. Sci.* **482**, 960 (2001).